Role of CBF transcription factors during long-term acclimation to high light and low temperature in two ecotypes of a winter annual

christopher baker[1], Jared Stewart[2], Cynthia Amstutz[1], Jeffrey Johnson[1], Lindsey Ching[1], Krishna Niyogi[1], William W. Adams[3], and Barbara Demmig-Adams[3]

[1]University of California Berkeley
[2]USDA-ARS Plains Area
[3]University of Colorado Boulder

July 20, 2020

Abstract

When grown under cool temperature, winter annuals respond with not only enhanced freezing tolerance but also photosynthetic upregulation. The role of the cold-induced C-repeat-Binding Factor (CBFs) in long-term maintenance of freezing tolerance and photosynthetic upregulation was examined in two Arabidopsis thaliana ecotypes adapted to differing climates (Italy = IT and Sweden = SW) as well as corresponding CBF-disabled mutant lines. Data on photosynthetic, morphological, and freezing-tolerance phenotypes as well as transcriptomic data were collected from plants grown for several weeks under controlled conditions with several combinations of temperature and light levels. Freezing tolerance in these acclimated plants depended strongly on CBFs in both SW and IT. In contrast, photosynthetic upregulation was the same, or modestly reduced, in cbf mutant versus parental lines of SW and IT, respectively. Physiological and transcriptomic data showed a consistent trend for a greater role of CBFs in cool-temperature-grown plants of IT versus SW. These features suggest that IT remained in a state of continuing CBF-related cold-acclimation even after weeks of acclimation, while SW entered a state of completed acclimation in which maintenance of photosynthetic upregulation no longer required CBF activation and maintenance of freezing tolerance was less dependent on CBF than in IT.

Introduction:

Acclimation to cool temperatures in winter annuals has two main components: (i) activation of survival traits, such as enhanced freezing tolerance, that permit survival during periods of subfreezing temperatures (Kang et al., 2013; Oakley, Ågren, Atchison, & Schemske, 2014; Thomashow, 1999; Zhen & Ungerer, 2008), and (ii) activation of growth-maintenance traits, such as photosynthetic upregulation, that facilitate continued growth and productivity on cool days (Anderson, Chow, & Park, 1995; Bode, Ivanov, & Hüner, 2016; Hüner et al., 2012; Huner, Öquist, & Sarhan, 1998). The mechanisms behind photosynthetic upregulation under winter conditions include synthesis of greater numbers of proteins involved in photosynthesis (Huner et al., 1993; Stitt & Hurry, 2002; Strand et al., 1999) as well as a greater capacity for sugar export from leaves (Adams, Cohu, Muller, & Demmig-Adams, 2013; Dumlao et al., 2012; Leonardos, Savitch, Huner, Öquist, & Grodzinski, 2003), which compensates for reduced enzyme activity under cool temperature. In addition, leaves of winter annuals grown in cool versus warm temperatures are thicker and contain more chloroplast-rich mesophyll cells per unit area (Adams, Stewart, Cohu, Muller, & Demmig-Adams, 2016; Cohu, Muller, Adams, & Demmig-Adams, 2014; Gorsuch, Pandey, & Atkin, 2010). By virtue of this enhancement of biochemical and structural features for photosynthesis and sugar export/transport, overwintering herbaceous plants are able to maintain high sugar production and transport to underground storage, while minimizing exposure of above-ground portions to freezing events by reducing leaf surface area (Eremina, Rozhon, & Poppenberger, 2016). Notably, a similar upregulation of photosynthetic capacity and leaf thickness takes place in many

species during acclimation to high growth-light intensity (Boardman, 1977; Gauhl, 1976; Munekage, Inoue, Yoneda, & Yokota, 2015; Yano & Terashima, 2004), including *Arabidopsis thaliana*(Hoshino, Yoshida, & Tsukaya, 2019; Stewart, Polutchko, Adams, & Demmig-Adams, 2017). Common regulatory networks may thus be involved in both cold and high-light acclimation, including the level of excitation pressure sensed by the chloroplast (Anderson et al., 1995; Hüner et al., 2012; Hüner, Dahal, Bode, Kurepin, & Ivanov, 2016).

It has been proposed that the transcription factor family of C-repeat-Binding Factors (CBFs) may link photosynthetic upregulation in response to growth under cool temperatures and/or high light intensity to enhanced freezing tolerance (Hüner et al., 2014, 2016). *A. thaliana* contains three tandemly duplicated *CBF* paralogs (*CBF1* , *CBF2* , and *CBF3* ; abbreviated to*CBF1–3* in this text) that are strongly induced by cold treatment and together direct many of the transcriptional and physiological changes necessary for enhanced freezing tolerance (Knight & Knight, 2012; Shi, Ding, & Yang, 2018; Thomashow, 1999). Laboratory studies have revealed largely overlapping functions for the CBF1–3 transcription factors as well as a requirement for combined loss-of-function mutations in all three genes for strongly reduced induction of freezing-tolerance genes and freezing tolerance itself (Gilmour, Fowler, & Thomashow, 2004; Jia et al., 2016; Park, Gilmour, Grumet, & Thomashow, 2018; Zhao et al., 2016). *CBF*over-expressing lines exhibited higher freezing tolerance as well as greater leaf thickness, chlorophyll levels, and photosynthetic rates per unit area even after growth under low light and warm conditions (Gilmour et al., 2004; Savitch et al., 2005). Thus, *CBF* overexpression is sufficient to induce both the survival trait of enhanced freezing tolerance and the productivity-maintenance trait of photosynthetic upregulation.

Following a five-year, reciprocal transplant investigation of two*A. thaliana* ecotypes (Ågren & Schemske, 2012), Rodasen-47 from Sweden (SW) and Castelnuovo-12 from Italy (IT), numerous studies provided insight into the ecophysiology and genetics underlying local adaptation in this model organism. Anatomical and physiological studies revealed that the Swedish ecotype exhibited much greater foliar phenotypic plasticity in response to both growth light intensity and temperature compared to the Italian ecotype (Adams, Cohu, Amiard, & Demmig-Adams, 2014; Adams et al., 2016; Adams, Stewart, Polutchko, & Demmig-Adams, 2018; Cohu, Muller, Demmig-Adams, & Adams, 2013a; Cohu, Muller, Stewart, Demmig-Adams, & Adams, 2013b; Stewart et al., 2015, 2016, 2017). The Swedish ecotype was also shown to have a greater tolerance to deep-freezing events relative to the Italian ecotype (Oakley et al., 2014; Park et al., 2018). The *CBF* s were identified as a QTL for fitness (Ågren et al., 2013) and freezing tolerance (Oakley et al., 2014), and subsequent work revealed that IT possesses an 8-bp deletion in its *CBF2* gene that renders the CBF2 transcription factor nonfunctional (Gehan et al., 2015). While IT exhibited greater freezing tolerance when transformed with the SW*CBF2* allele (Gehan et al., 2015), the loss of functional CBF2 in IT is not sufficient to account for its lower freezing tolerance relative to SW (Park et al., 2018).

In the present study, IT and SW were grown under several differing conditions using a factorial design of light intensity and temperature regimes. Transcriptome data from fully expanded leaves were generated to compare expression patterns of genes associated with freezing tolerance and photosynthesis, and chloroplast redox state (redox state of the primary electron acceptor of photosystem II, Q_A) was assessed to address the relationship between chloroplast excitation pressure and *CBF1–3* expression levels. Under the two most different growth conditions, the parental ecotypes were subsequently grown alongside their corresponding mutant lines that encode nonfunctional CBF1–3 proteins, it:*cbf123* and sw:*cbf123* , respectively, and a mutant line of SW that encodes a nonfunctional CBF2, sw:*cbf2* (Park et al., 2018). Fully expanded leaves of these plants were assayed for freezing tolerance, morphological and photosynthetic characteristics, and expression of genes associated with these phenotypic traits.

iv. a. Materials and Methods:

Plant material and growth conditions

Arabidopsis thaliana ecotypes IT (Castelnuovo-12 [ABRC stock number: CS98761], sub-line 24) and SW (Rodasen-47 [ABRC stock number: CS98762], sub-line 29) were grown from seed in Conviron E15 growth chambers (Controlled Environments Ltd., Manitoba, Canada) and then in Percival Scientific E36-HID

chambers (Perry, Iowa) alongside sw:*cbf2* , sw:*cbf123,* and it:*cbf123* mutant lines, which were generated via CRISPR/Cas9 and plants used in this study were confirmed by Sanger sequencing to carry the expected mutations. For more information on the ecotypes, see (Oakley et al., 2014; Stewart et al., 2017). The following four growth conditions—based on a factorial design of contrasting light intensities and temperature regimes—were employed: low light, warm temperatures (LLW; 9-h photoperiods of 100 μmol photons m^{-2} s^{-1} and 25°C/20°C [light/dark] leaf temperatures), low light, cool temperatures (LLC; 9-h photoperiods of 100 μmol photons $m^{-2}s^{-1}$ and 16°C/12.5°C [light/dark] leaf temperatures), high light, warm temperatures (HLW; 9-h photoperiods of 1000 μmol photons m^{-2} s^{-1} and 25°C/20°C [light/dark] leaf temperatures), and high light, cool temperatures (HLC; 9-h photoperiods of 1000 μmol photons m^{-2} s^{-1} and 14°C/12.5°C [light/dark] leaf temperatures). All plants were grown from seeds that were kept in H_2O at 4°C for 4 days and then germinated in six-pack seed-starting trays containing 50-mL soil (Fafard Growing Mix 2; Sun Gro Horticulture, Massachusetts, USA) under 9-h photoperiods of either 100 (LLW and LLC) or 1000 (HLW and HLC) μmol photons m^{-2} s^{-1} and a common air temperature regime of 25°C during the photoperiod and 20°C during the dark period. Following germination, individual seedlings were transplanted with 50-mL soil from their respective cells into larger (2.9-L) pots. Following this transplant, seedlings to be grown under LLW were kept at the air temperature at which they germinated (i.e., 25°C/20°C [light/dark] and 9-h photoperiods of 100 μmol photons m^{-2} s^{-1}), and seedlings to be grown in HLW were transferred to a constant air temperature of 20°C so that the leaf temperatures were 25°C during the photoperiod and 20°C during the dark period. Seedlings to be grown in LLC were transferred to 16°C/15°C (light/dark) for 7 days and then to 16°C/12.5°C (light/dark) air temperatures, and HLC plants were transferred to a constant air temperature of 15°C for 7 days and then to an 8°C/12.5°C (light/dark) air temperature regime so that the leaf temperatures were 14°C during the photoperiod and 12.5°C during the dark period. The leaves of LLW and LLC plants did not differ from the respective air temperatures. Plants were grown under their respective final growth conditions for several weeks and received water daily with nutrients added every other day as previously described (Stewart et al., 2015).

Leaf phenotypic traits

Leaf photosynthetic capacity was determined as light- and CO_2-saturated oxygen evolution with leaf disc oxygen electrodes (Hansatech Instruments Ltd., Norfolk, UK) as previously described (Delieu & Walker, 1981). The reduction state of the primary electron acceptor of photosystem II, Q_A, was assessed via measurements of chlorophyll fluorescence using a pulse-amplitude-modulated (PAM) chlorophyll fluorometer (FMS2; Hansatech Instruments Ltd., Norfolk, UK). Leaves were darkened for 20 min, exposed to a far-red light of 0.6 μmol photons $m^{-2}s^{-1}$ for 5 min, and then subjected to 5-min exposures of increasing light intensities. At the end of each 5-min exposure, steady-state fluorescence (Strand et al., 1999) were recorded, maximum fluorescence levels (F_m´) were obtained by applying a saturating pulse of light (0.8 s of 3000 μmol photons m^{-2} s^{-1}), and then minimum fluorescence levels (F_o´) were recorded by briefly darkening the leaf. Q_A reduction state was calculated as $1 - q_L = (1/F_s - 1/F_m')/(1/F_o' - 1/F_m')$. Measurements on LLW plants were conducted in the laboratory at ambient temperature (approximately 22degC), and measurements on HLC plants were conducted inside the growth chamber in which they were grown (with an air temperature of 8degC). Chlorophyll *a* and *b* content was determined via high-performance liquid chromatography as previously described (Stewart et al., 2015) or via spectrophotometry as previously described (Arnon, 1949) from leaf discs (0.30 cm^2) collected at the end of the 15-h dark period.

Leaf dry mass was measured with an A-160 balance (Denver Instruments Company, Denver, CO, USA) from leaf discs that were dried at 70degC for 7 d. For leaf-thickness measurements, leaves were embedded in 7% (w/v) agarose and sectioned into 80–100 μm thick sections using a 752/M vibroslice tissue cutter (Campden Instruments Limited, Loughborough, England). Sections were stained with 0.02% toluidine blue O for 30 s, and images were taken approximately 150 μm away from the mid-vein (where no major veins or trichomes were present) with an AxioImager (Zeiss, Oberkochen, Germany) coupled with a MicroPublisher color camera (QImaging, Surrey, Canada). Leaf thickness was quantified for 10 representative sections of each plant (i.e., 10 technical replicates for each biological replicate) using ImageJ (Schneider et al., 2012).

Freezing-tolerance assays were performed as previously described (Thalhammer, Hincha, & Zuther, 2014). Leaves in 300 µl of deionized H_2O where subjected to subfreezing temperatures using an Arctic A25 refrigerated water bath (Thermo Fisher Scientific, Waltham, MA) and a cooling rate of 4°C h^{-1}. Electrical conductivity was measured using an Exstik II probe (Extech Instruments, Waltham, MA). The data for each replicate were fitted to a four-parameter logistic model, and lethal freezing temperatures (LT_{50}) values were determined as the inflection points from these models. Maximal photosystem II efficiency in darkness was assessed via measurements of chlorophyll fluorescence with an Imaging-PAM Maxi (Walz, Effeltrich, Germany). Minimal fluorescence levels (F_o) were recorded after a 20-min dark period at room temperature following the freezing treatments, and then maximal fluorescence levels (F_m) were recorded by applying a pulse of saturating light (1800 µmol photons $m^{-2}s^{-1}$). Maximal photosystem II efficiency was calculated as $F_v/F_m = (F_m - F_o)/F_m$, and false-colored images of F_v/F_m were generated using ImageJ (Schneider, Rasband, & Eliceiri, 2012).

Gene Expression Analysis Using Real-Time qPCR.

RNA extraction, cDNA synthesis, and qPCR were performed as previously described (Wakao et al., 2014). All primer pairs were confirmed as having 90–105% amplification efficiency and linear amplification within their dynamic range in experimental samples using serial dilutions of cDNA prior to experiments. Relative transcript levels were calculated by the ΔΔCt method (Livak & Schmittgen, 2001) using*PEX4* (AT5G25760) as the internal reference. *PEX4* , a peroxisomal ubiquitin-conjugating enzyme, is an established RT-qPCR internal reference (Dekkers et al., 2012) and was confirmed in the RNAseq dataset to have constant expression levels in all conditions and ecotypes. Primers were designed using Primer3 (Untergasser et al., 2012) against the 3´-UTR of each gene to avoid binding to off-target paralogous genes. A single peak in melt-curve analysis with a unique melting temperature was observed for each amplicon, verifying that off-target amplification of paralogous genes was negligible.

RNAseq library preparation and analysis

Two flash-frozen leaf discs of 0.73 cm^2 collected at the end of the 15-h dark period were homogenized in liquid nitrogen by bead beating, and RNA was extracted and DNase-treated using the Qiagen RNeasy Plant Mini Kit (Qiagen, Germany). Integrity of purified RNA was validated using a 2100 Bioanalyzer (Agilent, California, USA), and concentration determined using a QuBit fluorometer (Thermo Fisher Scientific, Massachusetts, USA). Plant rRNA was depleted from 2 µg of purified RNA using the RiboZero rRNA removal kit for Plants (Illumina, California, USA). Barcoded cDNA libraries were generated from our rRNA-depleted RNA samples using the TruSeq RNA library preparation kit (Illumina, California, USA). Sequencing of barcoded cDNA libraries was performed at the Vincent J. Coates Genomics Sequencing Laboratory using a HiSeq2500 platform using 50 bp single-end reads (Illumina, California, USA).

Statistical analyses

RNAseq analysis was performed using the genomic analysis tools available through Galaxy (Afgan et al., 2018). Quality of RNAseq runs was validated by FastQC and adapter sequences were clipped using FASTQ (Gordon, 2010). Reads were mapped to the *A. thaliana* reference genome (TAIR10), and preliminary differential expression analysis was conducted using HISAT and StringTie (Kim, Landmead, & Salzberg, 2015; Pertea et al., 2015). Differential expression analysis was conducted using DESeq2 as well as the calculation of adjusted *p*- values, which limit high false positive discovery rates due to multiple testing (Love, Huber, & Anders, 2014). Data can be accessed on the Gene Expression Omnibus at GSE154349. Log2 fold-changes were transformed with the rlog (regularized log) function to minimize variance caused by low expression genes, then clustered and plotted using pheatmap (Kolde, 2018). In pheatmap, each sample was clustered on the horizontal axis based on the similarity of its transcriptome to the 23 other transcriptomes. On the vertical axis, individual genes were clustered based on the similarity of their expression profile across the 24 samples to the expression profile of other genes.

Comparisons of two means were evaluated via Student's *t* tests, and comparisons of multiple means evaluated via one-way analysis of variance (ANOVA) and post hoc Tukey–Kramer Honestly Significant Differences

(HSD) tests. Nonlinear curves were generated using 3-parameter exponential and 4-parameter logistic models. All statistical analyses, excluding those of RNAseq data, were conducted using JMP software (Pro 15.0.0; SAS Institute Inc., Cary, NC, USA).

iv. b. Results:

Interaction of growth environment with ecotype in shaping photosynthetic characteristics, expression of CBF genes, and leaf transcriptome

The highest photosynthetic capacity (Fig. 1a), leaf dry mass per area (Fig. 1b), and chlorophyll $a + b$ (Fig. 1c) were achieved under HLC (high light, cool temperature growth conditions). While photosynthetic capacity and leaf dry mass per area were also higher in HLW (high light, warm temperature growth conditions), chlorophyll $a + b$ levels remained similar to those under LLW conditions (low light, warm temperature growth conditions). Chlorophyll a / b ratios responded similarly to growth light conditions, with a strong ecotypic difference of higher chlorophyll a / b in IT versus SW under HLW but not HLC (Fig. 1d). Significant ecotype-specific differences were also observed in terms of higher photosynthetic capacity in SW under HLC and HLW (Fig. 1a), higher leaf dry mass per area in SW under HLC (Fig. 1b), and higher chlorophyll $a + b$ in SW under all conditions tested (Fig. 1c). In both ecotypes, the strongest *CBF1–3* transcript expression was also achieved in HLC (Fig. 2). As observed for photosynthetic capacity and leaf dry mass per area, *CBF1* and *CBF3* expression were greater in the SW versus IT HLC plants, but this pattern was somewhat different in LLC (low light, cool temperature growth conditions), under which the IT moderately induced *CBF1–3* while SW did not induce *CBF1–3* (Fig. 2).

Growth under HLC relative to LLW also induced sweeping changes in the leaf transcriptome in both ecotypes (Fig. 3). 2086 and 2176 genes were induced under HLC in IT and SW, respectively, with an adjusted p -value of less than 0.01 and a minimum fold-change of 2 (Table S1, S2). Similar numbers of genes were downregulated under HLC versus LLW, i.e., 2073 and 1992 genes for IT and SW, respectively (Table S3, S4). All three biological replicates co-clustered for both ecotypes grown under each of the four conditions upon hierarchical clustering, and the transcriptomic response of IT and SW in HLC conditions co-branched (Fig. 3a). This co-branching of HLC transcriptomes of the two ecotypes was due at least in part to large blocks of co-clustering genes that were specifically induced under HLC (HLC-specific genes) and downregulated under HLC (HLC-downregulated genes) in both ecotypes (Fig. 3a, Table S5-S7). HLC-specific induced genes were strongly enriched for a number of the Gene Ontology (GO) categories, of which the most enriched three categories were starch catabolism (GO:0005983), cold acclimation (GO:0009631), and protein refolding (GO:0042026) (Table S8). Similarly, GO analysis revealed pathways repressed specifically in HLC. For instance, the three most strongly over-represented pathways among genes specifically downregulated in HLC were water transport (GO:0006833), auxin polar transport (GO:0009926), and cytokinin-activated signaling pathways (GO:0009736) (Table S9).

Photosynthesis-related genes tended to have unique expression patterns in each ecotype under HLC. Photosynthesis-related genes tended to be downregulated under HLC in IT and upregulated in SW. Genes specifically downregulated in IT under HLC were in the categories of light harvesting in photosystem I (GO:0009768), light reaction (GO:0019684), and photosynthesis (GO:0015979) (Fig. 3b, Table S10-S12). In contrast, genes induced specifically in SW under HLC were enriched for both photosynthesis (GO:0015979), plastid organization (GO:0009657), and antioxidant biosynthesis pathways (GO:0006766) GO categories (Table S13-S15). The photosynthesis-related genes selectively upregulated in SW under HLC included multiple genes involved in the Calvin-Benson-Bassham cycle, cyclic electron flow around PSI, and chlorophyll and tocopherol biosynthesis (Fig. 3c).

Genes induced under HLC were also enriched for genes constitutively induced in *CBF* overexpression lines (Park et al., 2018), with p -values of 10^{-66} and 10^{-38} for IT and SW, respectively (Fig. 3d, Table S16). IT in LLC was the only other case where significant overlap with this set of ectopically expressed CBF-dependent genes was seen (p -value = 3.0×10^{-14}). Genes induced under HLC in both ecotypes, as well as genes induced in IT in LLC, were also enriched for genes downregulated in it:*cbf123* and sw:*cbf123* following sudden transfer

from warm growth conditions to 4°C for 24 h (Park et al., 2018), with p -values of 10^{-53}, 10^{-19} and 0.003, respectively (Table S17).

The response of chloroplast redox state to experimental exposure to different light intensities was ascertained in leaves of plants acclimated to HLC and LLW. Q_A reduction state was similar in the two ecotypes under LLW across a range of light intensities (Fig. 4a), with both ecotypes already exhibiting relatively high Q_A reduction states under relatively low light intensities. In addition, HLC plants of both ecotypes exhibited consistently lower Q_A reduction states than the LLW plants (Fig. 4a,b). The light response of Q_A reduction state differed between HLC in IT and SW, with SW exhibiting a significantly lower Q_A reduction state (more oxidized Q_A) than IT at higher light intensities (Fig. 4b).

Impact of CBFs on freezing tolerance and gene expression under LLW versus HLC

Freezing tolerance was significantly lower in plants acclimated to LLW versus HLC (Fig. 5a,b), with an LT_{50} near -5.6ºC for all five genotypes in LLW (Fig. 5a). For HLC plants, LT_{50} of freezing tolerance in sw:*cbf123* was lower by 3.5ºC relative to the SW and sw:*cbf2* lines (Fig. 5b). Similarly, LT_{50} of HLC plants was lower by 3.4ºC in it:*cbf123* relative to IT. This reduced freezing tolerance in the sw:*cbf123* and it:*cbf123* lines was accompanied by more pronounced freezing-induced depression of PSII efficiency F_v/F_m (Fig. 5c). At the same time, the greater freezing tolerance in HLC versus LLW for it:*cbf123* and sw:*cbf123* lines indicated some contribution from*CBF1–3* -independent freezing-tolerance mechanisms.

At the molecular level, induction of selected CBF- regulated genes was strongly inhibited in it:*cbf123* and sw:*cbf123* under HLC (Fig. 6). Five genes were chosen for assaying by RT-qPCR based*(i)* on prior demonstration of their regulation by *CBF1–3*using short-term cold shifts and *(ii)* demonstrated function in cold acclimation or cold-induced signaling. These five genes were Ser/Thr kinase *CIPK25* (AT5G25110), freezing-tolerance-related proteins *COR78* (AT5G52310), *LTI30* (AT3G50970),*COR15A* (AT2G42540), and *GOLS3* (AT1G09350). All five genes were induced under HLC in both parental ecotypes and exhibited strongly reduced induction under HLC in the it:*cbf123* and sw:*cbf123*lines (Fig. 6a–e). Two of the five genes, *COR15A* and*GolS3* , also had weakly attenuated induction in sw:*cbf2*relative to SW under HLC (Fig. 6d,e).

Impact of cbf deficiency on photosynthesis and leaf morphology in SW and IT under HLC

The impact of the *cbf123* mutation on photosynthetic and leaf-morphological traits was ecotype-specific under HLC. Strikingly, the sw:*cbf123* null mutant exhibited no significant differences under HLC in photosynthetic capacity, chlorophyll a + $b$per unit area, dry leaf mass per unit area, leaf thickness, or rosette diameter relative to SW (Fig. 7-9, Table 2). In contrast, the it:*cbf123* mutant in HLC showed modestly, but significantly, lower levels of these five traits relative to IT. Photosynthetic capacity (Fig. 7a) was 27% lower in HLC plants of it:*cbf123* relative to IT and leaf thickness (Fig. 8b-e) was 32% lower (Fig. 8a), with$p$-values of 0.0043 and 0.0042, respectively. Dry leaf mass per unit area and chlorophyll a + b levels per unit area were also modestly lower in it:*cbf123* relative to IT in HLC, with$p$ -values of 0.000021 and 0.0082, respectively (Fig. 7b,c). Differences in photosynthetic capacity, dry mass per leaf area, and chlorophyll a + b levels per unit area between it:*cbf123* and its parental ecotype were specific to HLC and not observed under LLW (Fig. 7). Another trait altered by the *cbf123*mutation in HLC plants of lT but not of SW was rosette diameter that was significantly larger in it:*cbf123* versus IT under HLC (Fig. 9 & Fig. S1). Lastly, there were no significant differences between the*cbf* mutants relative to their parental ecotypes in Q_A redox state (data not shown) or chlorophyll*a/b* ratio (Fig. 7d) under the growth and measurement regimes tested.

Beyond freezing tolerance: CBF regulon genes involved in HLC acclimation

Six IT-specific CBF regulon genes under HLC were confirmed by RT-qPCR (Fig. 10). Putative IT-specific CBF regulon genes under HLC were selected by two criteria, i.e., *(i)* as having been defined as a CBF-target gene in prior work (Park et al., 2018) and *(ii)*showing strong induction under HLC in IT. From among 31 genes that satisfied both criteria, nine were selected for validation by RT-qPCR with priority given to genes with protein domains or linked to a role in photosynthetic or leaf-morphological acclimation phenotypes. Genes confirmed as IT-specific CBF regulon genes under HLC, i.e., attenuated in it:*cbf123*

relative to IT but unchanged in sw:*cbf123*relative to SW, included sucrose synthase *SUS1* (AT5G20830), growth regulator *EGR2* (AT5G27930), and four strongly HLC-induced genes in both ecotypes with no known functions, including*RCI2A* (AT3G05880), AT5G44565, AT1G13930, and*LCR69* (AT2G02100). Three of the nine candidate genes tested for IT-specific CBF regulation had significantly lower expression in the*cbf 123* mutants of not only IT but also SW relative to their respective parental ecotype under HLC and are thus not IT-specific CBF regulon genes under HLC (Fig. S2).

iv. c. Discussion:

Common responses of the two ecotypes to high light and/or low temperature growth

Both *A. thaliana* ecotypes exhibited strong and significant upregulation of photosynthetic capacity in response to growth and development under HLW and to an even greater extent under HLC, a common response to low temperature or winter conditions in herbaceous winter annuals and biennials (Adams et al., 2013; Cohu et al., 2013b, 2014; Muller et al., 2014). This upregulation of photosynthetic capacity is part of a suite of acclimatory responses that support the ability to persist and thrive during winter. These responses included greater leaf mass per area, associated with more mesophyll cells and more chlorophyll per leaf area. The upregulation of photosynthesis coupled with the observed upregulation of genes involved in starch catabolism likely work synergistically to increase freezing tolerance through an elevated level of sugars that serve as cryoprotectants (Castonguay, Bertrand, Michaud, & Laberge, 2011; Strimbeck, Kjellsen, Schaberg, & Murakami, 2007).

The upregulation of photosynthetic capacity observed in both ecotypes in response to growth under high light and/or low temperature was previously shown to be accompanied by upregulation of foliar minor vein features of the phloem associated with an increased capacity for sugar export from the leaves (Adams et al. 2013, 2014, 2016, 2018; Cohu et al., 2013b; Stewart et al. 2016, 2017). On the other hand, acclimation to low versus high temperature also resulted in lower rates of transpiration and foliar vascular features (lower vein density and fewer xylem cells per minor vein) associated with a diminished capacity to distribute water to the leaves (Adams et al., 2016, 2018; Stewart et al., 2016). This latter result is consistent with the downregulation of genes associated with water transport and polar transport of auxin observed in response to growth under HLC in the present study. Vascular tissue formation in *A. thaliana* leaves (and thus vein density) as well as xylem differentiation is influenced by auxin synthesis and transport (Baylis, Cierlik, Sundberg, & Mattsson, 2013; Biedroñ & Banasiak, 2018; Fàbregas et al., 2015; Marcos & Berleth, 2014). There is, furthermore, a general consensus that vascular patterning arises from not only auxins but also their interaction with cytokinins (Etchells & Turner, 2017), the signaling pathways for which were found to be downregulated under HLC in the present study. Moreover, the development of xylem is a specific target of cytokinins (Kondo, Tamaki, & Fukuda, 2014).

Ecotype-specific responses to HLC growth for photosynthesis

While both IT and SW exhibited strong photosynthetic upregulation and transcriptomic differential regulation in HLC (with ˜6.5% of total leaf transcriptome induced and ˜6.1% downregulated relative to LLW), the marked ecotype-specific difference between two ecotypes under HLC in the expression of genes related to photosynthesis is consistent with the greater upregulation of photosynthesis in SW compared to IT in response to both high light and low temperature (Adams et al., 2014, 2016, 2018; Cohu et al., 2013b; Stewart et al., 2015, 2016, 2017). Genes activated in SW under HLC included genes involved in carbon assimilation and aspects of photoprotective energy dissipation via antioxidants and cyclic electron flow around PSI. These gene expression responses mirrored the higher photosynthetic capacity, higher chlorophyll $a+ b$ per unit area and more oxidized Q_A reduction state of SW versus IT in HLC. In contrast, the downregulation of genes involved in light harvesting in IT under HLC suggest that IT avoids excess light by reducing light-collection capacity rather than solely upregulating photosynthesis and photoprotective energy dissipation as seen in SW. These transcriptomic findings are consistent with the more highly reduced Q_A state, lower chlorophyll $a + b$ per unit per area, and higher chlorophyll a/b ratio (indicative of preferential degradation of the outer, chlorophyll$b$ -containing light-harvesting complexes) in IT versus SW under HLC.

Ecotype-specific responses to HLC growth for CBFs and CBF-regulated genes

The fact that the strongest induction of *CBF1-3* was achieved in both ecotypes under HLC indicates a synergistic effect of cool temperature and high light on *CBF1-3* induction. Elevated excitation pressure in the chloroplast may contribute to maintenance of elevated *CBF1-3* expression during long-term growth in HLC (Hüner et al., 2012; Hüner et al., 2016). Other possible contributing signals include tetrapyrrole Mg-ProtoIX-mediated retrograde signaling that impacts *CBF1-3* expression levels in specific mutant backgrounds (Lee & Thomashow, 2012; Noren et al., 2016). Ecotypic differences presumably also shape how HL-dependent signals are translated to*CBF1-3* induction. For instance, the finding that SW in HLC maintained a more oxidized Q_A state under experimental exposure to high light relative to IT in HLC is consistent with other phenotypic measures that indicate superior adaptation of SW to either high light or cold temperature than IT (Adams et al., 2014, 2016, 2018; Ågren & Schemske, 2012; Agrena, Oakley, McKay, Lovell, & Schemske, 2013; Cohu et al. 2013a,b; Oakley et al., 2014; Park et al., 2018; Stewart et al., 2015, 2016, 2017).

CBF1-3 are essential for long term maintenance of freezing tolerance in both ecotypes

The present finding that *CBF1-3* are essential to the full induction of freezing tolerance in the SW and IT ecotypes under HLC confirms their importance in *A. thaliana* as a key survival trait for overwintering plants. Previous studies showed that CBFs are essential for full induction of freezing tolerance in mature *A. thaliana* plants grown under warm conditions and transferred in one step to chilling conditions (Jia et al., 2016; Park et al., 2018; Zhao et al., 2016). The present study on plants grown from seed under differing temperature regimes demonstrates that CBFs also have an essential role in the long-term maintenance of elevated freezing tolerance. Moreover, just as was concluded from short-term studies on warm-grown *cbf*mutants abruptly transferred to cold conditions (Jia et al., 2016; Park et al., 2018; Zhao et al., 2016), both CBF-dependent and CBF-independent pathways also appear to be required for long-term freezing tolerance in HLC plants – as illustrated here by the moderately enhanced freezing tolerance in both it:*cbf123* and sw:*cbf123* under HLC versus LLW. This finding is also consistent with the observation that gene expression of CBF-target genes under HLC was strongly reduced, but not fully blocked, in *cbf123* triple mutants in the present study. Furthermore, the contribution of the CBF-dependent pathway to freezing tolerance after long-term growth under HLC was similar in both ecotypes (reduction of LT_{50} of freezing tolerance by 3.5 ºC and 3.4ºC under HLC in it:*cbf123* and sw:*cbf123* versus IT and SW, respectively). These findings indicate that the greater freezing tolerance of SW versus IT in HLC is due to CBF-independent pathways contributing to freezing tolerance (see also Park et al., 2018).

The absence of a clear effect under HLC in the sw:*cbf2* mutant is best explained by the impact of paralog compensation (Gilmour et al., 2004; Jia et al., 2016; Park et al., 2018; Zhao et al., 2016), i.e., functionally overlapping components that can partly compensate for each other's loss. The observation in the present study of stronger induction of many CBF-target genes under HLC in IT with its pre-existing*cbf2* mutation relative to SW could also be interpreted in the context of paralog compensation by *CBF1* and *CBF3* in a*cbf2* mutant background. Several independent *A. thaliana*lineages evolved loss-of-function mutations in individual *CBF*genes without apparent severe adverse effects on survival in regions with mild winters (Kang et al., 2013; Monroe et al., 2016). The full suite of *CBF1–3* may thus only be required for tolerance to colder conditions than used here (daytime air temperature of 8ºC and leaf temperature of ˜14 ºC).

However, paralog compensation among *CBF1–3* does not explain the observed significant induction of CBF-target genes and moderately elevated freezing tolerance of *cbf123* mutants in HLC, i.e., completely CBF-independent induction of some level of freezing tolerance. The concept of paralog compensation can also apply to entire gene families that may functionally overlap and compensate for each other's loss. *CBF1–3* belong to the ERF/AP2 A-1 subfamily that includes three additional members located outside the *CBF1–3*gene locus in *A. thaliana* (Mizoi, Shinozaki, & Yamaguchi-Shinozaki, 2012). However, these three other ERF/AP2 A-1 subfamily members (*DDF1,* AT1G12610; *DDF2* , AT1G63030;*CBF4* , AT5G51990) are not expressed at detectable levels in leaf tissue of IT or SW under any of the four growth regimes. Additionally, Park et al. (2018) observed no induction of these three genes in the it:*cbf123* and sw:*cbf123* in their various cold treatments. It is thus unlikely that paralog compensation accounts for the CBF-independent induction of

freezing observed in *cbf123* mutants. Instead, the present findings suggest involvement of unrelated signaling networks.

Ecotype-specific role for CBF1–3 in photosynthetic upregulation under HLC

The finding that, in contrast to freezing tolerance, photosynthetic upregulation under HLC was not inhibited in sw:*cbf2* or sw:*cbf123* , and was only modestly reduced in it:*cbf123*needs to be examined in the context of the strong constitutive photosynthetic upregulation observed upon over-expression of *CBF*paralogs (Hüner et al., 2014; Savitch et al., 2005). Photosynthetic upregulation, a developmental process involving changes at the organelle, cell, tissue, and whole plant levels (Hoshino et al., 2019; Yano & Terashima, 2004), is likely to involve multiple regulatory pathways. For example, blue-light photoreceptor signaling and foliar sucrose levels (Hoshino et al., 2019; Katagiri et al., 2016; Kozuka, Kong, Doi, Shimazaki, & Nagatani, 2011; Lopez-Juez, Bowyer, & Sakai, 2007) make contributions to increases in leaf thickness in HL-grown plants of a similar magnitude as those observed for CBF-dependent leaf thickening in the it:*cbf123* mutant under HLC. The present findings indicate that light-responsive signaling pathways with overlapping functions can fully compensate for the loss of*CBF1–3* in the sw:*cbf2* and sw:*cbf123* . Such alternative signaling pathways could thus include photoreceptors, photosynthetic sugar and redox signals, and phytohormone signals. Since loss of CBF activity in the it:*cbf123* mutant under HLC resulted in a modest increase in the temperature at which electrolyte leakage occurred as well as a significantly lower capacity for photosynthesis, both photosynthetic upregulation and long-term freezing tolerance in IT appear to be more dependent on CBF transcriptional activity than in SW. Taking the present results from long-term HLC acclimation and previous results on short-term transfer to cold conditions together, we suggest an obligatory role of *CBF1–3* as first-wave responders to abrupt chilling conditions (Fowler & Thomashow, 2002), and an apparent continuous engagement of IT in early-phase acclimation even after weeks of growth under HLC. In contrast, SW may achieve a state of complete cold acclimation, where *CBF1–3* transcriptional activity becomes entirely dispensable to maintaining photosynthetic upregulation – and partly dispensable to the maintenance of elevated freezing tolerance. This novel hypothesis of a more complete acclimation to HLC in SW (but not IT) is also consistent with the stronger photosynthetic upregulation and less elevated Q_A reduction state of SW in HLC.

The present comparative transcriptomic analysis of two ecotypes thus lends further support to a greater relative importance of *CBF*genes for long-term growth under HLC in IT versus SW, as had also been suggested for sudden transfer of warm-grown plants to chilling conditions but lower light intensity than used in the present study (Park et al., 2018; Sanderson et al., 2020). This is also supported by the finding that, among all pairings of ecotype x growth conditions in the present study, the largest percentage of CBF-target genes was induced in HLC-grown IT (Supplemental Tables). For example, 78.9% of CBF-target genes defined as genes constitutively induced in *CBF*overexpression lines were induced in HLC-grown IT, compared to only 49.3% in SW. While a hypothetical alternative explanation for this result would be transcriptional network divergence of CBF-regulated genes between SW and IT resulting in underestimation of CBF target genes in SW HLC plants, this explanation can be ruled out since Park et al., (2018) defined CBF regulons specific to IT and SW and all cross-comparisons to these gene lists consistently showed a greater percentage of CBF-target genes induced in HLC-grown IT (c.f., supplemental tables on CBF target genes). In summary, our evidence at the transcriptomic and physiological levels points towards a consistent trend of the CBF-dependent pathway having a greater ongoing role during long-term growth under HLC in IT versus SW, which might have been unexpected given the naturally occurring *cbf2* mutation in the IT background.

Identification of CBF-target genes that may contribute to photosynthetic upregulation

The ecotype-dependent effect on photosynthetic upregulation in the*cbf123* mutants presented an opportunity to identify CBF regulon genes potentially contributing to photosynthetic upregulation. CBF-regulated genes linked to photosynthetic upregulation under HLC should be strongly induced in the parental ecotypes, and based on the above discussion, exhibit reduced expression only in the it:*cbf123* mutant and not the sw:*cbf123* mutant. Two examples of genes that follow this expression pattern were*SUS1* (AT5G20830) and *EGR2* (AT5G27930). *SUS1* is a sucrose synthase not required for sucrose accumulation under conditions favorable

for growth, but strongly induced under several abiotic-stress conditions (Barratt et al., 2009; Bieniawska et al., 2007; Branco-Price, Kawaguchi, Ferreira, & Bailey-Serres, 2005; Kilian et al., 2007). Recent evidence linked high foliar sucrose levels to increased cell height in leaves grown under high light (Hoshino et al., 2019; Katagiri et al., 2016), which may be mediated by greater rates of endocycle reduplication of DNA (amplification of genome copy number in the absence of cell division) in palisade cells contributing to cell size expansion (Katagiri et al., 2016). In this context, it should be noted that *CBF* over-expressing lines exhibited increased leaf thickness and accumulation of soluble sugars, including sucrose, under LLW (Gilmour et al., 2004; Savitch et al., 2005).

The fact that it:*cbf123* plants had larger rosettes relative to IT in HLC may also be associated with the regulation of cell elongation and growth. Decreased rates of cell elongation during leaf development is likely a key component of how *A. thaliana* reduces rosette expansion under winter conditions to reduce foliar freezing damage (Hoshino et al., 2019; Yano & Terashima, 2004). *EGR2,* another confirmed IT-specific CBF target gene under HLC, is a negative regulator of growth that controls cytoskeletal-mediated vesicle trafficking to the plasma membrane (Bhaskara, Wen, Nguyen, & Verslues, 2017). Over-expression of *EGR2* was sufficient to reduce cell expansion and generate smaller rosettes, whereas *egr2* null mutants had enhanced cell elongation and larger rosettes (Bhaskara et al., 2017). Furthermore, post-translational modification of EGR2 under chilling stress induced *CBF1–3* expression (Ding et al., 2019), suggesting that *EGR2* may be a regulatory link between CBF transcriptional activity and whole-plant changes in rosette growth under HLC. Overall, the resource of IT-specific CBF-regulated genes under HLC, including*EGR2, SUS1,* and the four additional genes shown here to be IT-specific, may help define regulatory controls on photosynthetic upregulation to overwintering conditions. We hope that future work will seek further mechanistic insight into the ecotype-specific transcriptional control of photosynthetic pathways in response to growth environment, perhaps through phenotyping and transcriptionally profiling of Recombinant Inbred Line populations developed for these two populations under LLW and HLC conditions (Ågren et al., 2013).

v. Acknowledgements:

The lines *sw:cbf2, sw:cbf123,* and *it:cbf123* were generously provided by Professor Michael Thomashow at Michigan State University. This work was supported by the Gordon and Betty Moore Foundation through Grant GBMF 2550.03 to the Life Sciences Research Foundation [to C.R.B]. K.K.N. is an investigator of the Howard Hughes Medical Institute. This work was also supported by the National Science Foundation [DEB-1022236 to B.D.-A. and W.W.A., IOS-1907338 to J.J.S.]; and the University of Colorado.

vi. References:

Adams, W. W. III, Cohu, C. M., Muller, O., & Demmig-Adams, B. (2013). Foliar phloem infrastructure in support of photosynthesis.*Frontiers in Plant Science,* 4, 194.

Adams, W. W. III, Cohu, C. M., Amiard, V., & Demmig-Adams, B. (2014). Associations between phloem-cell wall ingrowths in minor veins and maximal photosynthesis rate. *Frontiers in Plant Science* , 5, 24.

Adams, W. W. III, Stewart, J. J., Cohu, C. M., Muller, O., & Demmig-Adams, B. (2016). Habitat temperature and precipitation of*Arabidopsis thaliana* ecotypes determine the response of foliar vasculature, photosynthesis, and transpiration to growth temperature.*Frontiers in Plant Science* , 7, 1026.

Adams, W. W. III, Stewart, J. J., Polutchko, S. K., & Demmig-Adams, B. (2018) Leaf vasculature and the upper limit of photosynthesis. In Adams, W. W. III & Terashima, I. (eds) The Leaf: A Platform for Performing Photosynthesis. Advances in Photosynthesis and Respiration, Vol. 44, Springer: Cham. pp. 27-54.

Afgan, E., Baker, D., Batut, B., van den Beek, M., Bouvier, D., Cech, M., . . . Blankenberg, D. (2018). The Galaxy platform for accessible, reproducible and collaborative biomedical analyses: 2018 update.*Nucleic Acids Research,* 46(W1), W537-W544.

Anderson, J. M., Chow, W. S., & Park, Y. I. (1995). The grand design of photosynthesis: acclimation of the photosynthetic apparatus to environmental cues. *Photosynthesis Research,* 46(1-2), 129-139.

Arnon, D. I. (1949). Copper enzymes in isolated chloroplasts - polyphenoloxidase in *Beta-vulgaris* . *Plant Physiology,*24(1), 1-15.

Ågren, J., & Schemske, D. W. (2012). Reciprocal transplants demonstrate strong adaptive differentiation of the model organism *Arabidopsis thaliana* in its native range. *New Phytologist,* 194(4), 1112-1122.

Ågren, J., Oakley, C. G., McKay, J. K., Lovell, J. T., & Schemske, D. W. (2013). Genetic mapping of adaptation reveals fitness tradeoffs in*Arabidopsis thaliana* . *Proceedings of the National Academy of Sciences of the United States of America,* 110(52), 21077-21082.

Barratt, D. H. P., Derbyshire, P., Findlay, K., Pike, M., Wellner, N., Lunn, J., . . . Smith, A. M. (2009). Normal growth of *Arabidopsis*requires cytosolic invertase but not sucrose synthase. *Proceedings of the National Academy of Sciences of the United States of America,*106(31), 13124-13129.

Baylis, T., Cierlik, I., Sundberg, E., Mattsson, J. (2013). *SHORT INTERDODES/STYLISH* genes, regulators of auxin biosynthesis, are involved in leaf vein development in *Arabidopsis thaliana* .*New Phytologist* , 197(3), 737-750.

Bhaskara, G. B., Wen, T. N., Nguyen, T. T., & Verslues, P. E. (2017). Protein phosphatase 2Cs and microtubule-associated stress protein 1 control microtubule stability, plant growth, and drought response.*Plant Cell,* 29(1), 169-191.

Biedroñ , M., & Banasiak, A. (2018). Auxin-mediated regulation of vascular patterning in *Arabidopsis thaliana* leaves. *Plant Cell Reports,* 37(9), 1215-1229.

Bieniawska, Z., Barratt, D. H. P., Garlick, A. P., Thole, V., Kruger, N. J., Martin, C., . . . Smith, A. M. (2007). Analysis of the sucrose synthase gene family in *Arabidopsis* . *Plant Journal,* 49(5), 810-828.

Boardman, N. K. (1977). Comparative photosynthesis of sun and shade plants. *Annual Review of Plant Physiology,* 28, 355-377.

Bode, R., Ivanov, A. G., & Hüner, N. P. A (2016). Global transcriptome analyses provide evidence that chloroplast redox state contributes to intracellular as well as long-distance signalling in response to stress and acclimation in *Arabidopsis* . *Photosynthesis Research,*128(3), 287-312.

Branco-Price, C., Kawaguchi, R., Ferreira, R. B., & Bailey-Serres, J. (2005). Genome-wide analysis of transcript abundance and translation in arabidopsis seedlings subjected to oxygen deprivation. *Annals of Botany, 96* (4), 647-660.

Castonguay, Y., Bertrand, A., Michaud, R., & Laberge, S. (2011). Cold-induced biochemical and molecular changes in alafalfa populations selectively improved for freezing tolerance. *Crop Physiology & Metabolism* , 51(5), 2132-2144.

Cohu, C. M., Muller, O., Adams, W. W. III, & Demmig-Adams, B. (2014). Leaf anatomical and photosynthetic acclimation to cool temperature and high light in two winter versus two summer annuals. *Physiologia Plantarum,* 152(1), 164-173.

Cohu, C. M., Muller, O., Demmig-Adams, B., & Adams, W. W. III (2013a). Minor loading vein acclimation for three *Arabidopsis thaliana*ecotypes in response to growth under different temperature and light regimes. *Frontiers in Plant Science* , 4, 240.

Cohu, C. M., Muller, O., Stewart, J. J., Demmig-Adams, B., & Adams, W. W. III (2013b). Association between minor loading vein architecture and light- and CO_2-saturated rates of photosynthetic oxygen evolution among *Arabidopsis thaliana* ecotypes from different latitudes. *Frontiers in Plant Science,* 4, 264.

Dekkers, B. J., Willems, L., Bassel, G. W., van Bolderen-Veldkamp, R. P., Ligterink, W., Hilhorst, H. W., & Bentsink, L. (2012). Identification of reference genes for RT-qPCR expression analysis in*Arabidopsis* and tomato seeds. *Plant and Cell Physiology,*53(1), 28-37.

Delieu, T., & Walker, D. A. (1981). Polarographic measurement of photosynthetic oxygen evolution by leaf discs. *New Phytologist,*89(2), 165-178.

Ding, Y., Lv, J., Shi, Y., Gao, J., Hua, J., Song, C., . . . Yang, S. (2019). EGR2 phosphatase regulates OST1 kinase activity and freezing tolerance in *Arabidopsis* . *European Molecular Biology Orgranization Journal,* 38(1), e99819.

Dumlao, M. R., Darehshouri, A., Cohu, C. M., Muller, O., Mathias, J., Adams, W. W. III, & Demmig-Adams, B. (2012). Low temperature acclimation of photosynthetic capacity and leaf morphology in the context of phloem loading type. *Photosynthesis Research,*113(1-3), 181-189.

Eremina, M., Rozhon, W., & Poppenberger, B. (2016). Hormonal control of cold stress responses in plants. *Cell Molecular Life Sciences,*73(4), 797-810.

Etchells, J. P., & Turner, S. R. (2017). Realizing pipe dreams - a detailed picture of vascular development. *Journal of Experimental Botany* , 68(1), 1-4.

Fàbregas, N., Formosa-Jordan, P., Confraria, A., Siligato, R., Alonso, J. M., Swarup, R., Bennett, M. J., Pekka Mähönen, A., Caño-Delgado, A. I., & Ibañes, M. (2015). Auxin influx carriers control vascular patterning and xylem differentiation in *Arabidopsis thaliana* .*PLoS Genetics* , 11(4), e1005183.

Fowler, S., & Thomashow, M. F. (2002). *Arabidopsis* transcriptome profiling indicates that multiple regulatory pathways are activated during cold acclimation in addition to the CBF cold response pathway.*Plant Cell,* 14(8), 1675-1690.

Gauhl, E. (1976). Photosynthetic response to varying light intensity in ecotypes of *Solanum-dulcamara* L. from shaded and exposed habitats. *Oecologia,* 22(3), 275-286.

Gehan, M. A., Park, S., Gilmour, S. J., An, C., Lee, C. M., & Thomashow, M. F. (2015). Natural variation in the C-repeat binding factor cold response pathway correlates with local adaptation of*Arabidopsis* ecotypes. *Plant Journal,* 84(4), 682-693.

Gilmour, S. J., Fowler, S. G., & Thomashow, M. F. (2004).*Arabidopsis* transcriptional activators CBF1, CBF2, and CBF3 have matching functional activities. *Plant Molecular Biology,* 54(5), 767-781.

Gordon, A. (2010). FASTQ: A short-reads pre-processing tools. Retrieved from http://hannonlab.cshl.edu/fastx_toolkit/.

Gorsuch, P. A., Pandey, S., & Atkin, O. K. (2010). Temporal heterogeneity of cold acclimation phenotypes in *Arabidopsis*leaves. *Plant Cell and Environment,* 33(2), 244-258.

Hoshino, R., Yoshida, Y., & Tsukaya, H. (2019). Multiple steps of leaf thickening during sun-leaf formation in *Arabidopsis* . *Plant Journal* . 100(4), 738-737.

Huner, N. P. A., Öquist, G., Hurry, V. M., Krol, M., Falk, S., & Griffith, M. (1993). photosynthesis, photoinhibition and low-temperature acclimation in cold tolerant plants. *Photosynthesis Research,*37(1), 19-39.

Huner, N. P. A., Öquist, G., & Sarhan, F. (1998). Energy balance and acclimation to light and cold. *Trends in Plant Science,* 3(6), 224-230.

Hüner, N. P. A., Bode, R., Dahal, K., Hollis, L., Rosso, D., Krol, M., & Ivanov, A. G. (2012). Chloroplast redox imbalance governs phenotypic plasticity: the "grand design of photosynthesis" revisited.*Frontiers in Plant Sciences,* 3, 255.

Hüner, N. P. A., Dahal, K., Kurepin, L. V., Savitch, L., Singh, J., Ivanov, A. G., . . . Sarhan, F. (2014). Potential for increased photosynthetic performance and crop productivity in response to climate change: role of CBFs and gibberellic acid. *Frontiers in Chemistry,* 2, 18.

Hüner, N. P. A., Dahal, K., Bode, R., Kurepin, L. V., & Ivanov, A. G. (2016). Photosynthetic acclimation, vernalization, crop productivity and 'the grand design of photosynthesis'. *Journal of Plant Physiology,* 203, 29-43.

Jia, Y., Ding, Y., Shi, Y., Zhang, X., Gong, Z., & Yang, S. (2016). The cbfs triple mutants reveal the essential functions of CBFs in cold acclimation and allow the definition of CBF regulons in*Arabidopsis* . *New Phytologist,* 212(2), 345-353.

Kang, J., Zhang, H., Sun, T., Shi, Y., Wang, J., Zhang, B., . . . Gu, H. (2013). Natural variation of *C-repeat-binding factor*(*CBF* s) genes is a major cause of divergence in freezing tolerance among a group of *Arabidopsis thaliana* populations along the Yangtze River in China. *New Phytologist,* 199(4), 1069-1080.

Katagiri, Y., Hasegawa, J., Fujikura, U., Hoshino, R., Matsunaga, S., & Tsukaya, H. (2016). The coordination of ploidy and cell size differs between cell layers in leaves. *Development,* 143(7), 1120-1125.

Kilian, J., Whitehead, D., Horak, J., Wanke, D., Weinl, S., Batistic, O., . . . Harter, K. (2007). The AtGenExpress global stress expression data set: protocols, evaluation and model data analysis of UV-B light, drought and cold stress responses. *Plant Journal,* 50(2), 347-363.

Kim, D., Landmead, B., & Salzberg, S. L. (2015). HISAT: a fast spliced aligner with low memory requirements. *Nature Methods,* 12(4), 357-360.

Knight, M. R., & Knight, H. (2012). Low-temperature perception leading to gene expression and cold tolerance in higher plants. *New Phytologist,* 195(4), 737-751.

Kolde, R. (2018). pheatmap: Pretty Heatmaps. *R package version 1.0.10.* Retrieved from https://CRAN.R-project.org/package=pheatmap.

Kondo, Y., Tamaki, T., & Fukuda, H. (2014). Regulation of xylem fate.*Frontiers in Plant Science* , 5, 315.

Kozuka, T., Kong, S. G., Doi, M., Shimazaki, K., & Nagatani, A. (2011). Tissue-autonomous promotion of palisade cell development by Phototropin 2 in *Arabidopsis* . *Plant Cell,* 23(10), 3684-3695.

Lee, C. M., & Thomashow, M. F. (2012). Photoperiodic regulation of the C-repeat binding factor (CBF) cold acclimation pathway and freezing tolerance in *Arabidopsis thaliana* . *Proceedings of the National Academy of Sciences of the United States of America,*109(37), 15054-15059.

Leonardos, E. D., Savitch, L. V., Huner, N. P. A., Öquist, G., & Grodzinski, B. (2003). Daily photosynthetic and C-export patterns in winter wheat leaves during cold stress and acclimation.*Physiologia Plantarum* , 117(4), 521-531.

Livak, K. J., & Schmittgen, T. D. (2001). Analysis of relative gene expression data using real-time quantitative PCR and the $2^{-\Delta\Delta\hat{}}{}_{\mathrm{T}}$ method. *Methods,*25(4), 402-408.

Lopez-Juez, E., Bowyer, J. R., & Sakai, T. (2007). Distinct leaf developmental and gene expression responses to light quantity depend on blue-photoreceptor or plastid-derived signals, and can occur in the absence of phototropins. *Planta,* 227(1), 113-123.

Love, M. I., Huber, W., & Anders, S. (2014). Moderated estimation of fold change and dispersion for RNA-seq data with DESeq2. *Genome Biology,* 15(12), 550.

Marcos, D., & Berleth, T. (2014). Dynamic auxin transport patterns preceding vein formation revealed by live-imaging of Arabidopsis leaf primordia. *Frontiers in Plant Science* , 5, 235.

McKhann, H. I., Gery, C., Berard, A., Leveque, S., Zuther, E., Hincha, D. K., . . . Teoule, E. (2008). Natural variation in CBF gene sequence, gene expression and freezing tolerance in the Versailles core collection of *Arabidopsis thaliana* . *BioMed Central Plant Biology,* 8, 105.

Mizoi, J., Shinozaki, K., & Yamaguchi-Shinozaki, K. (2012). AP2/ERF family transcription factors in plant abiotic stress responses.*Biochimica et Biophysica Acta,* 1819(2), 86-96.

Monroe, J. G., McGovern, C., Lasky, J. R., Grogan, K., Beck, J., & Mckay, J. K. (2016). Adaptation to warmer climates by parallel functional evolution of CBF genes in *Arabidopsis thaliana* .*Molecular Ecology,* 25(15), 3632-3644.

Muller, O., Stewart, J. J., Cohu, C. M., Polutchko, S. K., Demmig-Adams, B., & Adams, W. W. III (2014). Leaf architectural, vascular, and photosynthetic acclimation to temperature in two biennials.*Physiologia Plantarum* , 152(4), 763-772.

Munekage, Y. N., Inoue, S., Yoneda, Y., & Yokota, A. (2015). Distinct palisade tissue development processes promoted by leaf autonomous signalling and long-distance signalling in Arabidopsis thaliana.*Plant Cell and Environment* , 38(6), 1116-1126.

Noren, L., Kindgren, P., Stachula, P., Ruhl, M., Eriksson, M. E., Hurry, V., & Strand, Å. (2016). Circadian and plastid signaling pathways are integrated to ensure correct expression of the CBF and COR genes during photoperiodic growth. *Plant Physiology* , 171(2), 1392-1406.

Oakley, C. G., Ågren, J., Atchison, R. A., & Schemske, D. W. (2014). QTL mapping of freezing tolerance: links to fitness and adaptive trade-offs. *Molecular Ecology* , 23(17), 4304-4315.

Park, S., Gilmour, S. J., Grumet, R., & Thomashow, M. F. (2018). CBF-dependent and CBF-independent regulatory pathways contribute to the differences in freezing tolerance and cold-regulated gene expression of two *Arabidopsis* ecotypes locally adapted to sites in Sweden and Italy. *PLoS One* , 13(12), e0207723.

Pertea, M., Pertea, G. M., Antonescu, C. M., Chang, T. C., Mendell, J. T., & Salzberg, S. L. (2015). StringTie enables improved reconstruction of a transcriptome from RNA-seq reads. *Nature Biotechnology* , 33(3), 290-295.

Sanderson, B. J., Park, S., Jameel, M. I., Kraft, J. C., Thomashow, M. F., Schemske, D. W., & Oakley, C. G. (2020). Genetic and physiological mechanisms of freezing tolerance in locally adapted populations of a winter annual. *American Journal of Botany* , 107(2), 250-261.

Savitch, L. V., Allard, G., Seki, M., Robert, L. S., Tinker, N. A., Huner, N. P. A., . . . Singh, J. (2005). The effect of overexpression of two *Brassica CBF/DREB1* -like transcription factors on photosynthetic capacity and freezing tolerance in *Brassica napus* .*Plant and Cell Physiology* , 46(9), 1525-1539.

Schneider, C. A., Rasband, W. S., & Eliceiri, K. W. (2012). NIH Image to ImageJ: 25 years of image analysis. *Nature Methods* , 9(7), 671-675.

Shi, Y., Ding, Y., & Yang, S. (2018). Molecular regulation of CBF signaling in cold acclimation. *Trends in Plant Science* , 23(7), 623-637.

Stewart, J. J., Adams, W. W. III, Cohu, C. M., Polutchko, S. K., Lombardi, E. M., & Demmig-Adams, B. (2015). Differences in light-harvesting, acclimation to growth-light environment, and leaf structural development between Swedish and Italian ecotypes of*Arabidopsis thaliana* . *Planta* , 242(6), 1277-1290.

Stewart, J. J., Demmig-Adams, B., Cohu, C. M., Wenzl, C. A., Muller, O., & Adams, W. W. III (2016). Growth temperature impact on leaf form and function in *Arabidopsis thaliana* ecotypes from northern and southern Europe. *Plant Cell and Environiment* , 39(7), 1549-1558.

Stewart, J. J., Polutchko, S. K., Adams, W. W. III, & Demmig-Adams, B. (2017). Acclimation of Swedish and Italian ecotypes of *Arabidopsis thaliana* to light intensity. *Photosynthesis Research* , 134(2), 215-229.

Stitt, M., & Hurry, V. (2002). A plant for all seasons: alterations in photosynthetic carbon metabolism during cold acclimation in Arabidopsis.*Current Opinion in Plant Biology* , 5(3), 199-206.

Strand, Å., Hurry, V., Henkes, S., Huner, N., Gustafsson, P., Gardeström, P., & Stitt, M. (1999). Acclimation of *Arabidopsis*leaves developing at low temperatures. Increasing cytoplasmic volume accompanies increased activities of enzymes in the Calvin cycle and in the sucrose-biosynthesis pathway. *Plant Physiology* , 119(4), 1387-1397.

Strimbeck, G. R., Kjellsen, T. D., Schaberg, P. G., & Murakami, P. F. (2007). Cold in the common garden: comparative low-temperature tolerance of boreal and temperate conifers foliage. *Trees,* 21(5), 557-567.

Thalhammer, A., Hincha, D. K., & Zuther, E. (2014). Measuring freezing tolerance: electrolyte leakage and chlorophyll fluorescence assays.*Plant Cold Acclimation: Methods and Protocols* , 1166, 15-24.

Thomashow, M. F. (1999). PLANT COLD ACCLIMATION: freezing tolerance genes and regulatory mechanisms. *Annual Review of Plant Physiology and Plant Molecular Biology, 50* , 571-599.

Untergasser, A., Cutcutache, I., Koressaar, T., Ye, J., Faircloth, B. C., Remm, M., & Rozen, S. G. (2012). Primer3-new capabilities and interfaces. *Nucleic Acids Research* , 40(15), e115.

Wakao, S., Chin, B. L., Ledford, H. K., Dent, R. M., Casero, D., Pellegrini, M., . . . Niyogi, K. K. (2014). Phosphoprotein SAK1 is a regulator of acclimation to singlet oxygen in *Chlamydomonas reinhardtii* . *eLife* , 3, e02286.

Yano, S., & Terashima, I. (2004). Developmental process of sun and shade leaves in *Chenopodium album* L. *Plant Cell and Environment* , 27(6), 781-793.

Zhao, C., Zhang, Z., Xie, S., Si, T., Li, Y., & Zhu, J. K. (2016). Mutational evidence for the critical role of CBF transcription factors in cold acclimation in *Arabidopsis* . *Plant Physiology* , 171(4), 2744-2759.

Zhen, Y., & Ungerer, M. C. (2008). Clinal variation in freezing tolerance among natural accessions of *Arabidopsis thaliana* .*New Phytologist* , 177(2), 419-427.

viii. Figure Legends:

Figure 1. (a) Photosynthetic capacity (i.e., maximal light- and CO_2-saturated rate of oxygen evolution) per leaf area, (b) leaf dry mass per area, (c) level of chlorophyll $a + b$per leaf area, and (d) chlorophyll a/b ratio in leaves of IT (red columns) and SW (blue columns) plants that were grown in low light/warm temperature growth conditions (LLW), low light/cool temperature growth conditions (LLC), high light/warm temperature growth conditions (HLW), or high light/cool temperature growth conditions (HLC). Mean values ± standard deviations ($n = 3$ or 4); groups that share the same letters are not considered statistically different, and groups that do not share the same letters are considered statistically different based on one-way ANOVA and post hoc Tukey–Kramer HSD tests.

Figure 2. Relative transcript abundance of (a) *CBF1* , (b)*CBF2* , and (c) *CBF3* in leaves of IT (red columns) and SW (blue columns) plants that were grown in LLW, LLC, HLW, or HLC. Values are presented relative to the expression level for each respective gene in the IT ecotype grown under LLW. Mean values ± standard deviations ($n = 3$); groups that share the same letters are not considered statistically different, and groups that do not share the same letters are considered statistically different based on one-way ANOVA and post hoc Tukey–Kramer HSD tests.

Figure 3. (a) Hierarchical clustering of the $\log_2$ expression data for 7,933 genes with an adjusted$P$- value below 0.01 in one of the pairwise comparisons for differential expression between ecotypes and growth conditions. The three biological replicates for each growth condition/ecotype set are shown as separate columns. (b-d) Log_2 expression data for IT and SW in HLC relative to LLW for (b) the subset of genes involved in light reactions of photosynthesis that were downregulated in IT under HLC, (c) the subset of genes involved in cyclic electron flow around PSI, Calvin-Benson-Bassham cycle, and chlorophyll biogenesis that were found to be induced in SW under HLC, and (d) CBF-regulated genes.

Figure 4. Reduction state of the primary electron acceptor of photosystem II, Q_A, quantified by chlorophyll fluorescence using the equation 1 - q_L, for IT (red circles) and SW (blue squares) in (a) LLW and (b) HLC. Mean values +- standard deviations ($n = 3$); statistically significant differences between ecotypes based on Student's t -tests are indicated with *asterisks* (* = $P < 0.05$, ** =$P < 0.01$, *** = $P < 0.001$);$n.s$. = not significantly different.

Figure 5. Cellular electrolyte leakage following exposures to freezing temperatures of IT (red circles), it:*cbf123* (light red circles), SW (blue squares), sw:*cbf2* (lighter blue squares), and sw:*cbf123* (lightest blue squares) in (a) LLW or (b) HLC, as well as (c) images of leaves following exposures to freezing temperatures with false colors based on photosystem II photochemical efficiency (as F_v/F_m) for HLC plants. For (a) and (b), mean values +- standard deviations ($n = 3$).

Figure 6. Transcript abundance for (a) *CIPK25,* (b)*COR78,* (c) *LTI30,* (d) *COR15a,* and (e) *GolS3*in leaves of IT (red columns), it:*cbf123* (light red columns), SW (blue columns), sw:*cbf2* (lighter blue columns), and sw:*cbf123* (lightest blue columns) plants that were grown in the LLW or HLC conditions. All values are normalized based on the expression levels of IT in LLW. Mean values +- standard deviations ($n = 3$); groups that share the same letters are not considered statistically different, and groups that do not share the same letters are considered statistically different based on one-way ANOVA and post-hoc Tukey–Kramer HSD tests.

Figure 7. (a) Photosynthetic capacity (i.e., light- and CO_2-saturated rate of oxygen evolution) per leaf area, (b) leaf dry mass per area, (c) level of chlorophyll $a + b$per leaf area, and (d) chlorophyll a/b ratio in leaves of IT (red columns), it:*cbf123* (light red columns), SW (blue columns), sw:*cbf2* (lighter blue columns), and sw:*cbf123* (lightest blue columns) plants that were grown in LLW or HLC. Mean values +- standard deviations ($n = 3$ to 5); Groups that share the same letters are not considered statistically different, and groups that do not share the same letters are considered statistically different based on one-way ANOVA and post-hoc Tukey–Kramer HSD tests.

Figure 8. (a) Leaf thickness of IT (red column), it:*cbf123* (light red column), SW (blue column), sw:*cbf2*(lighter blue column), and sw:*cbf123* (lightest blue column) plants that were grown in HLC, as well as representative images of leaf cross-sections for (b) IT, (c) it:*cbf123* , (d) SW, and (e) sw:*cbf123* . For (a), mean values +- standard deviations ($n = 3$); groups that share the same letters are not considered statistically different, and groups that do not share the same letters are considered statistically different based on one-way ANOVA and post-hoc Tukey–Kramer HSD tests.

Figure 9. (a) Rosette diameter of IT (red column), it:*cbf123* (light red column), SW (blue column), sw:*cbf2*(lighter blue column), and sw:*cbf123* (lightest blue column) after 40 days of growth in HLC, as well as images of representative (b) IT, (c) it:*cbf123* , (d) SW, and (e) sw:*cbf123* plants. For (a), mean values +- standard deviations ($n = 5$); groups that share the same letters are not considered statistically different, and groups that do not share the same letters are considered statistically different based on one-way ANOVA and post-hoc Tukey–Kramer HSD tests.

Figure 10. Relative transcript abundance for (a) *SUS1,*(b) *EGR2,* (c) *RCI2A,* (d) *AT5G44565,* (e)*AT1G13930* , and (f) *LCR69* in leaves of IT (red columns), it:*cbf123* (light red columns), SW (blue columns), and sw:*cbf123* (light blue columns) plants grown in LLW or HLC. All values are normalized based on the expression levels of IT in LLW. Mean values +- standard deviations ($n = 3$); groups that share the same letters are not considered statistically different, and groups that do not share the same letters are considered statistically different based on one-way ANOVA and post-hoc Tukey–Kramer HSD tests.

Supplementary information

i. Supplemental Figure and Table legends

Figure S1. Rosette diameter for IT (red columns), it:*cbf123* (light red columns), SW (blue columns), sw:*cbf2*(lighter blue columns), and sw:*cbf123* (lightest blue columns) plants after 32 days of growth in LLW. Mean values +- standard deviations ($n = 3$).

Figure S2. Relative transcript abundance of (a) *KIN2,*(b) *COR15B,* and (c) *AT1G21790* in leaves of IT (red columns), it:*cbf123* (light red columns), SW (blue columns), and sw:*cbf123* (light blue columns) under LLW and HLC. All values were normalized to expression levels in IT under LLW for the relevant gene. Mean values +- standard deviations ($n = 3$); groups that share the same letters are not considered statistically

different, and groups that do not share the same letters are considered statistically different based on one-way ANOVA and post-hoc Tukey–Kramer HSD tests.

Table S1. The 1992 genes downregulated in SW under HLC (minimum fold change of 2 and adjusted P -value of < 0.01).

Table S2. The 2073 genes downregulated in IT under HLC (minimum fold change of 2 and adjusted P -value of < 0.01).

Table S3. The 2176 genes upregulated in SW under HLC (minimum fold change of 2 and adjusted P -value of < 0.01).

Table S4. The 2086 genes upregulated in IT under HLC (minimum fold change of 2 and adjusted P -value of < 0.01).

Table S5. The 668 genes downregulated in both IT and SW under HLC (minimum fold change of 2 and adjusted P -value of < 0.01).

Table S6. The 753 genes upregulated in both IT and SW under HLC (minimum fold change of 2 and adjusted P -value of < 0.01).

Table S7. The 356 genes that co-clustered into the cluster labeled "HLC-Specific Group 1" and "HLC-Specific Group 2" in Fig. 3a.

Table S8. PANTHER Overrepresentation Test (Released 2019-07-11) on GO Ontology database (Released 2019-12-09) for genes upregulated in both IT and SW under HLC.

Table S9. PANTHER Overrepresentation Test (Released 2019-07-11) on GO Ontology database (Released 2019-12-09) for genes downregulated in both IT and SW under HLC.

Table S10. The 1405 genes downregulated specifically in IT under HLC (minimum fold change of 2 and adjusted P -value of < 0.01), 1323 genes upregulated specifically in HLC-grown IT plants (minimum fold change of 2 and adjusted P -value of < 0.01).

Table S11. PANTHER Overrepresentation Test (Released 2019-07-11) on GO Ontology database (Released 2019-12-09) for genes downregulated specifically in HLC-grown IT.

Table S12. Genes downregulated specifically in IT under HLC from four photosynthesis-related GO categories enriched in PANTHER Overrepresentation Test (photosynthesis (GO:0015979), photosynthesis, light reaction (GO:0019684), photosynthesis, light harvesting (GO:0009765), photosynthesis, light harvesting in photosystem I (GO:0009768) genes).

Table S13. The 1413 genes upregulated specifically in SW under HLC (minimum fold change of 2 and adjusted P -value of < 0.01) and the 1324 genes downregulated specifically in HLC-grown SW plants (minimum fold change of 2 and adjusted P -value of < 0.01).

Table S14. PANTHER Overrepresentation Test (Released 2019-07-11) on GO Ontology database (Released 2019-12-09) for genes upregulated specifically in SW under HLC .

Table S15. PANTHER Overrepresentation Test for genes upregulated specifically in SW under HLC (Photosynthesis (GO:0015979), plastid organization (GO:0009657), vitamin metabolic process (GO:0006766) genes).

Table S16. Comparison of transcriptomic data from four growth conditions for both ecotypes to genes reported to be over-expressed under low light and warm temperatures by Park, Gilmour, Grumet, & Thomashow (2018).

Table S17. Genes previously reported to be CBF-regulated—Comparison of transcriptomic data from four growth conditions for both ecotypes to genes identified as having diminished induction in it:*cbf123* and sw:*cbf123* mutants following a 24-hour 4degC treatment by Park, Gilmour, Grumet, & Thomashow (2018).

Hosted file

MaintextFigures.pdf available at https://authorea.com/users/343982/articles/470650-role-of-cbf-transcription-factors-during-long-term-acclimation-to-high-light-and-low-temperature-in-two-ecotypes-of-a-winter-annual

Figure 1

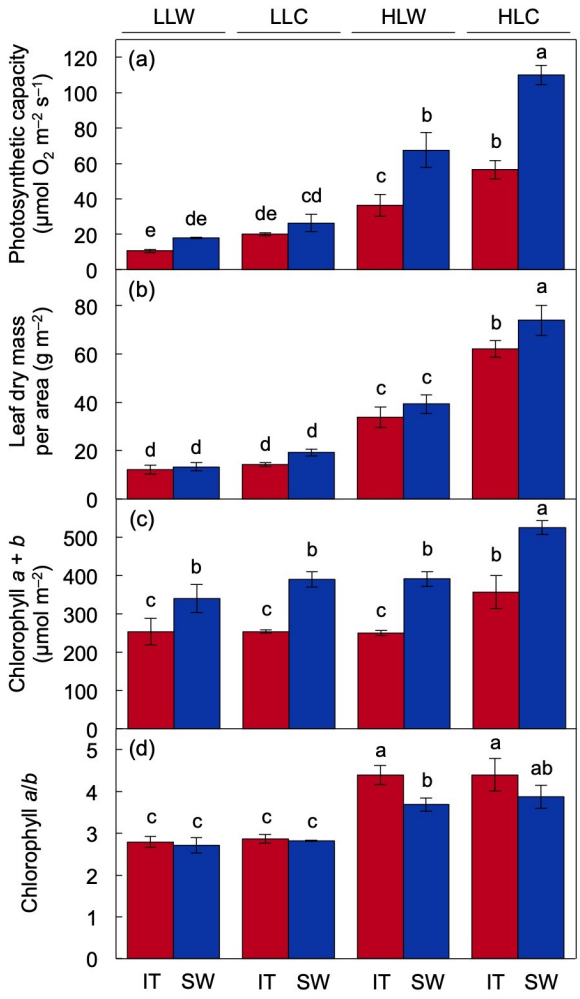

Hosted file

Supplemental_tables_PCE.xlsx available at https://authorea.com/users/343982/articles/470650-role-of-cbf-transcription-factors-during-long-term-acclimation-to-high-light-and-low-temperature-in-two-ecotypes-of-a-winter-annual

Hosted file

SupplementalFigures.pdf available at https://authorea.com/users/343982/articles/470650-

role-of-cbf-transcription-factors-during-long-term-acclimation-to-high-light-and-low-temperature-in-two-ecotypes-of-a-winter-annual